# MoLoRa: Intelligent Mobile Antenna System for Enhanced LoRa Reception in Urban Environments

Ningning Hou[1], Yifeng Wang[3], Xianjin Xia[2], Shiming Yu[2], Yuanqing Zheng[2], Tao Gu[1]
[1] Macquarie University, Sydney, Australia
[2] The Hong Kong Polytechnic University, Hong Kong SAR, China
[3] Carnegie Mellon University, Pittsburgh, PA, USA
{ningning.hou,tao.gu}@mq.edu.au,{xianjin.xia,csyqzheng}@polyu.edu.hk,
yifengw3@andrew.cmu.edu,shiming.yu@connect.polyu.hk

## ABSTRACT

LoRa technology promises to enable Internet of Things applications over large geographical areas. However, its performance is often hampered by poor channel quality in urban environments, where blockage and multipath effects are prevalent. Our study uncovers that a slight shift in the position or attitude of the receiving antenna can substantially improve the received signal quality. This phenomenon can be attributed to the rich multipath characteristics of wireless signal propagation in urban environments, wherein even small antenna movement can alter the dominant signal path or reduce the polarization angular difference between transceivers. Leveraging these key observations, we propose and implement MoLoRa, an intelligent mobile antenna system designed to enhance LoRa packet reception. At its core, MoLoRa represents the position and attitude of an antenna as a state and employs a statistical optimization method to search for states that offer optimal signal quality efficiently. Through extensive evaluation, we demonstrate that MoLoRa achieves a maximum Signal-to-Noise Ratio (SNR) gain of 13 dB in a few attempts, enabling formerly problematic blind spots to reconnect and strengthening links for other nodes.

## CCS CONCEPTS

• **Computer systems organization → Embedded and cyber-physical systems**.

## KEYWORDS

Internet of Things, LoRa, packet reception, mobile antenna

**ACM Reference Format:**
Ningning Hou, Yifeng Wang, Xianjin Xia, Shiming Yu, Yuanqing Zheng, Tao Gu. 2025. MoLoRa: Intelligent Mobile Antenna System for Enhanced LoRa Reception in Urban Environments. In *The 23rd ACM Conference on Embedded Networked Sensor Systems (SenSys '25), May 6–9, 2025, Irvine, CA, USA.* ACM, New York, NY, USA, 13 pages. https://doi.org/10.1145/3715014.3722075

## 1 INTRODUCTION

Low Power Wide Area Networks (LPWANs) have emerged as a new generation of wireless technology for connecting ubiquitous Internet-of-Things (IoT) applications over large areas [5, 22, 29–31, 40, 44, 50, 51, 56, 59, 61, 71, 78, 79, 82]. LoRa, as a representative LPWAN technology, utilizes Chirp Spread Spectrum (CSS) to enable data transmission over tens of kilometers with low-power consumption [4, 10, 52, 64].

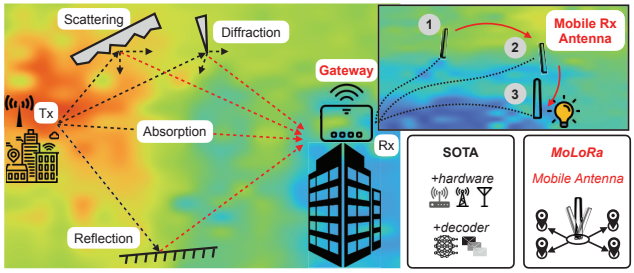


**Figure 1: The RF radiance in urban settings can be distorted by many factors, causing multipath and polarization mismatch at the receiver. MoLoRa moves an Rx antenna to find the optimal reception position and overcome polarization mismatch.**

Recent studies have shown that LoRa devices deployed in open rural areas achieve the advertised communication range [15, 18, 37]. However, urban environments, characterized by severe blockage and multipath effects, experience unsatisfactory communication distances, typically around 1 km or even shorter [28, 35, 58, 63, 81]. Importantly, blind spots may occur often in urban settings, resulting in reception and decoding failures even within sub-kilometer ranges.

Although several efforts have been made to enhance LoRa packet reception in urban environments, these approaches suffer from practical issues such as degraded data rates or increased hardware costs. As summarized in Table. 1, ADR mechanism sacrifices data rate and increases transmission power to improve reliability. XCopy [72] conducts sub-sample level synchronization, which is stringent and challenging for COTS devices, to coherently combine multiple identical packets received by a single antenna while Charm [8] and MALoRa [23] require multiple antennas to combine packets. Demeter [53] requires additional programmable antennas at each low-end LoRa node to adjust the polarization, which is not practical and backward compatible. Previous works [45] in WSN also proposed to use directional antenna and electronically-switched directional (ESD) antenna to improve signal quality. However, they are not capable of mitigating polarization misalignment.


*SenSys '25, May 6–9, 2025, Irvine, CA, USA*

ACM ISBN 979-8-4007-1479-5/2025/05
https://doi.org/10.1145/3715014.3722075

**Table 1: Qualitative comparison.**

| Method \ Feature | Data Rate | COTS Node | Single Antenna | Coarse Sync.[1] | SNR Gain |
|---|---|---|---|---|---|
| ADR | ↓ | ✔ | ✔ | ✔ | 2-3 dB |
| Charm[8] | – | ✔ | ✘ | ✘ | 1-3 dB |
| MALoRa[23] | – | ✔ | ✘ | ✔ | 1-6 dB |
| XCopy[72] | ↓ | ✔ | ✔ | ✘ | 3-10 dB |
| Demeter[53] | – | ✘ | ✔ | ✘ | 3-10 dB |
| **MoLoRa** | – | ✔ | ✔ | ✔ | 6-13 dB |

[1] Coarse sync refers to a synchronization process with relatively loose time requirements (resolution equals to or above sample-level).

We conducted in-field experiments to investigate blind spot problem in urban environments. A network with 30 LoRa nodes and a gateway is deployed in a dense urban area. Experiments reveal that many blind spots exist in urban environments even though there is a gateway nearby. We also observe that while some locations exhibit poor link quality, nearby areas have relatively good and stable link quality within certain time periods. These observations align with small-scale fading [38, 39, 49, 84, 86] of radio signal over a short distance. The variability can be attributed to the rich multipath in urban settings, where the creation of new non-line-of-sight paths can substantially enhance link quality. Therefore, one hypothesis is that a slight shift in the location of nodes or gateways (channel reciprocity) may alter the dominant path of the combined signal, leading to significant improvements in the received signal strength (RSS).

Another observation is that *the physical alignment of antennas in a transmitter-and-receiver pair does not necessarily guarantee optimal RSS*. Despite the assumption of polarization alignment when antennas are physically aligned, we find that environmental obstacles can induce angular twisting in the transmitted electromagnetic (EM) field. Similarly, as illustrated in Figure 1, signal reflections, scattering, diffraction, and absorption can lead to polarization misalignment at the receiver's antenna, degrading signal quality. Therefore, another hypothesis is that adjusting the antenna orientation can reduce the angular difference ($\theta$) between the EM fields of transmit and receive antennas, minimizing polarization loss and thereby improving signal quality.

These observations inspire us to explore the potential of a smart antenna by adjusting the **position and orientation** of a receiver's antenna to enhance packet reception. By enabling micro-mobility (*i.e.*, shifting to nearby positions and/or adopting new orientations), as illustrated in Figure1, blind spot nodes can seize opportunities to deliver packets successfully. Additionally, for nodes outside blind spots, fine-tuning the receiving antenna's position and orientation can further boost packet reception. This mechanism can also benefit downlink transmissions due to channel reciprocity.

Despite the benefits of enabling mobility for a receiving antenna, a crucial question arises: how can we determine the optimal state of an antenna? Although previous works [38, 39, 84] have discussed optimal placement of base station for wireless networks, they mainly focus on theoretical analysis and ray-tracing simulation, which overlook practical challenges (*e.g.*, polarization mismatch and real-time reaction) in system research, making them unsuitable for long range and complex urban LoRa networks. To find the optimal state, we cast this problem as an SNR maximization problem. We use the SNR of received packets as an indicator of signal quality and leverage a Bayesian optimization (BayesOpt)-based approach to identify the best state for receiving packets. Bayesian optimization has demonstrated its ability to effectively approximate real-world SNR distributions by leveraging previous exploration results [32]. However, unlike traditional BayesOpt which searches for a maximum or minimum, our goal is to find a state that provides satisfactory signal quality with minimal exploration efforts. This distinction arises due to the dynamic and complex nature of SNR distribution in space, where instant interference is challenging to model or predict using long-term historical data. Moreover, excessive exploration may yield diminishing marginal returns, further complicating the search for an appropriate state. Our design enables the antenna to reach a satisfactory state within just a few iterations, allowing the system to continually train the BayesOpt prediction model using previously received packets. Unlike traditional machine learning models [57, 68], which generally require extensive training before testing, our approach supports real-time packet reception and model training. This ensures no packets are wasted and maintains compatibility with all device classes in LoRa networks (Class A, B, and C) for gateway access. Besides, LoRa channel is relatively stable compared with other signals such as WiFi [25, 40]. This character makes our design feasible for real-world LoRa reception.

However, since LoRa nodes are distributed across various locations and experience distinct propagation paths, adjusting the position and orientation of a receiving antenna on a node-by-node basis is impractical and time-consuming. Furthermore, from a network perspective, this approach fails to support concurrent transmission. Fortunately, we note that some nodes may share similar optimal receiving states, allowing a gateway to group these states into clusters. Therefore, a gateway can coordinate the transmission of LoRa nodes by using beacons and ping slots of Class B devices and receive packets by transitioning between several representative states. This approach strikes a balance between efficiency and adaptability, offering promising potential for enhancing LoRa network performance in urban environments. For Class A and C nodes, our method can help a gateway antenna to select a state that satisfies the majority of nodes and avoid states with high probabilities of blind spots.

In this paper, we present MoLoRa, an intelligent mobile antenna system designed to enhance LoRa communication performance by dynamically adapting the position and orientation of the receiving antenna. To achieve this, MoLoRa harnesses a Bayesian optimization-based method to effectively learn complex environments between transceivers based on historical measurements, thereby automating the search for optimal states across multiple nodes. Additonally, MoLoRa is compatible with three device types in LoRa networks and it measures the packet SNR as an indicator of real-time channel condition. Our work complements the state-of-the-art by offering a solution that does not compromise data rates and can work with single-antenna COTS LoRa devices.

We build proof-of-concept prototypes of *MoLoRa* using various actuation devices, including low-cost and easy-to-setup actuation machines (*e.g.*, sliding track [83] and gimbal [7]), as well as high-end robot arms. Other low-cost devices such as Servo motors, stepper motors, DC motors with Gearbox, Pneumatic actuators, Soleno can also be used in practical applications. To evaluate MoLoRa's

performance, we conduct experiments in real-world urban environments using commodity off-the-shelf (COTS) LoRa nodes. Our experiment involves collecting and evaluating over 10,500 packets across different times and channel conditions. Results show that MoLoRa achieves 6 to 13 dB SNR gains on average after a few rounds of antenna adjustments, enabling most former blind spot nodes to successfully re-connect to a gateway. Our prototype with a sliding track and a gimbal also provide excellent performance enhancement.

In summary, this paper makes the following contributions:

- We investigate the impact of antenna position and orientation on received signal quality through comprehensive experiments, identifying a novel opportunity to enhance LoRa packet reception by enabling antenna mobility—a solution that is orthogonal to existing approaches in the LoRa literature.
- We design and implement a practical Bayesian optimization based antenna control algorithm to automate the rapid search for optimal antenna states that offer satisfactory signal quality with minimum exploration efforts.
- We build prototypes of MoLoRa with COTS actuation devices to facilitate the micro-mobility of the LoRa gateway's antenna. Experiment results demonstrate that MoLoRa can achieve up to a 13 dB increase in Signal-to-Noise Ratio (SNR) and a 50% boost in network throughput.

## 2 FEASIBILITY AND MOTIVATION

In this section, we study the feasibility of antenna mobility in improving signal qualities in urban environments.

### 2.1 Position of receiving antenna

**Experiment settings.** We conduct experiments in a practical LoRaWAN network deployed on a university campus, located at the heart of a metropolis representing a typical urban environment. For the convenience of experiments, we use a more flexible mobile antenna system as shown in Figure 10 (a). We use a commodity LoRa node (LoRa shield [9]) as a transmitter to transmit packets once a second. As for the receiver, we use a COTS gateway antenna (VERT900) and mount it to the gripper of a robot arm (JAKA Zu 3 [26]) with adjustable position and orientation. The robot arm's base remains stationary on a desktop and the arm's length, with a gripper of 1 m, allows the antenna to change its position within a hemisphere centered on the base. We conduct this experiment in an indoor environment. The distance between the transmitting LoRa node and the receiving antenna is approximately 50 m, separated by several walls and doors.

We conduct experiments to quantitatively study the effects of antenna position on the quality of received signals. In specific, we keep LoRa nodes' position and orientation unchanged and only change the position of the gateway's antenna while keeping its polarization direction fixed. We randomly select 16 positions within the ranges of the robot arm (*i.e.*, $< 3m^2$). We collect 20 packets at each position and calculate the average signal-to-noise ratio (SNR) of received packets. Figure 2 (a) represents the result. We observe that antenna positions greatly affect the receiving performance. For example, the medium SNR is as low as 8.4 dB at position #9, while it increases to 14.5 dB when the receiving antenna moves to position #16. Even though the changing of antenna position is relatively small compared to the long communication distance, such small changes in position cause significant SNR variations (6.1 dB in this example). This phenomenon encourages us to properly select positions for a receiving antenna to achieve good packet reception performance.

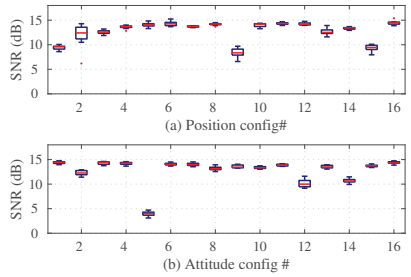


**Figure 2: Impact of different (a) positions and (b) orientations.**

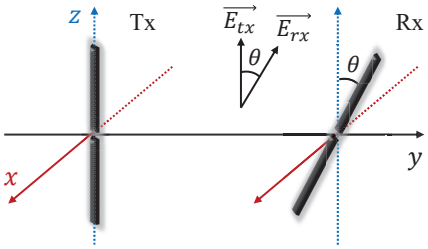


**Figure 3: Illustration of antenna polarization. Electric direction miss match ($\theta$) can cause polarization loss of power at the receiver.**

### 2.2 Polarization of antenna

Antenna polarization reflects the direction of the electromagnetic wave it emits or receives [27]. It is an important character of an antenna and has a significant impact on the received signal strength. To empirically study the impact of polarization on packet reception, we rotate the orientation of gateway's antenna uniformly to 16 different orientations within the plane perpendicular to the direction of electromagnetic wave, while keeping the antenna's position fixed. We collect 20 packets' SNR at each orientation and report results in Figure 2 (b). We can observe that polarization also affects signal's SNR. For instance, orientation #5 achieves the worst SNR of 4.5 dB, which is 10.4 dB lower than that of packets collected with orientation #1. Such a huge SNR variation is caused mainly by polarization misalignment since the position of the antenna is fixed. Our experiments show that the SNR variation induced by polarization mismatch (10.4 dB) can be even larger than that of the position change (6.1 dB), depending on the various channel conditions.

As the quality of received signal is affected by orientation of antenna, a natural question is: how can we decide the orientation to get the best signal quality? In theory, if polarization is not considered, the received signal power $P_r$ can be calculated with Friis

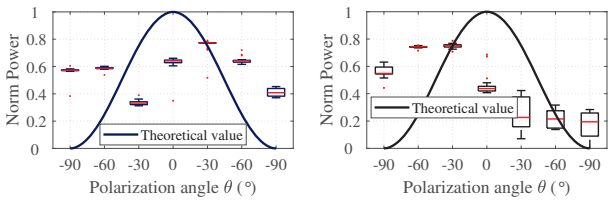


(a) Indoor (b) Outdoor

**Figure 4: Practical signal power is misaligned with theoretical power model in both (a) Indoor environment and (b) Outdoor environment.**

Transmission Formula [66]:

$$P_r = \frac{P_t G_t G_r \lambda^2}{(4\pi d)^2} \tag{1}$$

where $P_t$ is the transmission power, $G_t$ and $G_r$ are the gains of transceiver antennas respectively, $\lambda$ is the wavelength of signal, and $d$ is the distance between the transceiver. While antenna polarization is taken into consideration, a new term named *polarization loss factor* (PLF) [2, 54, 70] shall be used. PLF is generally defined as follows:

$$PLF = |\overrightarrow{E_{tx}} \cdot \overrightarrow{E_{rx}}|^2 = cos^2(\theta) \tag{2}$$

where $\theta$ is the angle between the unit electric direction vector of transmitting and receiving antennas ( $\overrightarrow{E_{tx}}$ and $\overrightarrow{E_{rx}}$) as shown in Figure 3. In the case of linear polarization, we just need to project the incident electric field onto the polarization axis of the antenna. The received signal power with polarization loss can be represented as

$$P_r(\theta) = P_r cos^2(\theta) \tag{3}$$

In this case, we expect that the maximum received signal power is obtained when the orientations of transmitter and receiver antennas are aligned (*i.e.*, $\theta = 0$).

However, in real-world implementation, we find it hard to achieve maximum SNR by physically aligning the transceiver's antenna. We conduct controlled experiments by varying the orientation shift angle $\theta$ while keeping the position fixed. We see from Figure 4 that the power measurement results differ significantly from the theoretical values in both indoor and outdoor settings. *The receiver's orientation with maximum signal power does not physically align with the transmitter's orientation.* Instead, the receiver reports the highest SNR when $\theta = -30^\circ$ in the indoor environment and $\theta = 30^\circ$ in the outdoor environment. A hypothetical reason is that the multi-path and signal blockages in real-world environments [2] can cause reflection, scattering, and diffraction, which fade the signal strength and distort the direction of the electric field. The RF radiance in space with blockages and multi-path does not fit the ideal RF radiance model. Thus, we cannot apply an ideal model like Eq. (3) to decide the best antenna orientation for a transceiver.

## 2.3 Motivation

The above experiments show that small changes in the position and orientation of a receiving antenna can indeed cause significant variations in the SNRs of received LoRa signals. Interestingly, the best SNR may not necessarily be obtained when the transmitter and receiver antennas are physically aligned. It calls for practical and adaptive approaches to adjust the antenna position and orientation. In LoRaWAN applications, low-cost LoRa nodes are typically deployed statically over large areas, and many of these nodes are not feasible for frequent access (*e.g.*, nodes located in pipelines or basements for oil or gas monitoring). It is challenging to impose the state adaption overhead on such low-cost and resource-constrained LoRa nodes. Conversely, LoRa gateways are usually tether-powered and have relatively sufficient resources to support antenna state optimization. Therefore, we choose to put the intelligence on gateways rather than end nodes.

The unique characteristics of LoRa communication also allow implementations of such an intelligent antenna: (1) Proved by prior studies [23, 72], the long-symbol and preamble structure of LoRa packets make it possible to detect LoRa signals and estimate SNRs accurately, even when the signal strength falls below noise floors. This enables a gateway to examine link conditions even for nodes located in blind spots. (2) The low duty cycles (*e.g.*, <1%) and low traffic rates of LoRaWANs leave large time intervals (*e.g.*, tens of seconds) between two transmissions of a node, providing sufficient time for antenna state selection and movements.

# 3 DESIGN

## 3.1 System overview

The key idea of MoLoRa is enabling antenna mobility to explore a better state for receiving packets instead of sticking to a fixed position. We term the specific position and orientation of an antenna as the antenna's *state*. The state is defined as a 6-tuple, ($x$, $y$, $z$, $\alpha$, $\beta$, $\gamma$), where $x$, $y$, $z$ denote the 3D antenna position and $\alpha$, $\beta$, $\gamma$ denote the roll, yaw, pitch of the antenna respectively. MoLoRa mounts a gateway antenna on a mobile actuation device. We first build the system with some easy-to-setup actuation devices and then move to a more powerful robot arm to achieve better performance.

**Actuator design.** Initially, we built the system with simple, easy-to-set-up actuation devices, *i.e.*, a sliding track ($10 USD) and a gimbal ($22 USD), which are combined with step or servo motors to control the antenna's position and orientation. We then extended our design to an advanced prototype using a robot arm to achieve enhanced flexibility and performance. Although the robot arm serves as an example of a sophisticated actuation device, MoLoRa's design remains compatible with more cost-effective alternatives, allowing users to choose according to their practical needs.

In our prototype, we choose an SDR receiver as the gateway to gain access to physical-layer raw data for ultra-weak packet detection, offering more experimental flexibility. In future implementations, this capability could be integrated directly into commercial off-the-shelf (COTS) gateways. Details on implementations and experiments with various actuation devices are provided in §4.3.7.

In LoRaWAN, Class A and Class C devices send uplink packets randomly, while Class B devices transmit periodically. MoLoRa first focuses on Class B nodes in this section, as their periodic transmissions allow for a more predictable optimization process, and then generalizes its functionality to handle Class A and C devices.

MoLoRa focuses on scenarios where a LoRa node reports sensor data (*e.g.*, temperature and humidity) periodically to a gateway.

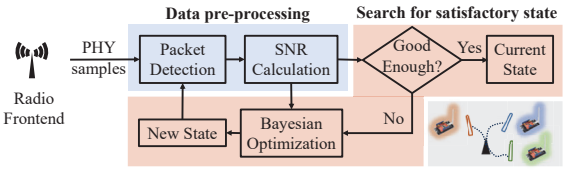


**Figure 5: *MoLoRa*'s high-level design: Separate modules handle data pre-processing, state optimization, and multi-node joint optimization for Class B devices.**

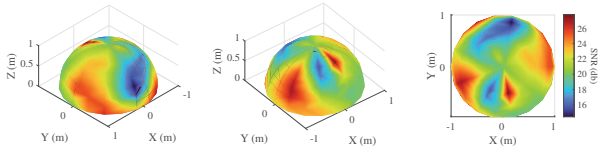


(a) 3D view 1 (b) 3D view 2 (c) 2D view

**Figure 6: Distribution of SNRs in an indoor scenario (Figure 10 (a)).**

Figure 5 shows MoLoRa's high-level design, which uses a mobile antenna for packet reception. It first detects the arrival of a packet and then calculates the signal-to-noise ratio (SNR) of the packet as an indicator of signal quality. If the signal quality is not good enough for packet demodulation or decoding, a BayesOpt-based method will be used to search for a satisfactory receiving state (antenna position and orientation). Otherwise, the antenna keeps receiving packets in the current state. Previous work [64] also report that many LoRa nodes share similar optimal receiving states in urban area. This encourages us to further coordinate the transmission of end nodes and extend MoLoRa to multiple nodes. Note that MoLoRa demodulates and decodes incoming packets as a commodity LoRa gateway.

## 3.2 Data pre-processing

The data pre-processing contains two phases:

**Packet detection.** Standard LoRa packet detection adopts a one-chirp detection window and signals the presence of a packet when 4 periodic peaks are detected after cross-correlation (CAD) or FFT on dechirped signal. However, this method struggles to detect extremely low-SNR packets from blind spots, even with the most aggressive ADR parameters.

MoLoRa leverages unique packet structure of LoRa to detect weak packets. In specific, LoRa preamble consists of several consecutive and identical base chirps, which can be added up within a larger detection window. Therefore, our packet detection module enlarges the detection window to combat noise by concentrating the energy of multiple chirps. The larger the detection window, the higher the energy peak of the targeted chirp signal. Theoretically, a combination of 4 chirps can achieve roughly 6 dB SNR gain for packet detection [23]. In our design, we use 8 base chirps in preamble and slide a detection window with length of 4 chirps. We configure the sliding step to 1 chirp to achieve high detection sensitivity as well as low energy consumption. We also signal the presence of a packet if 4 periodic peaks are detected.

**SNR calculation.** Once a packet is detected, MoLoRa needs to calculate the SNR of packets and then feed the result to the following state optimization module. Intuitively, we can represent the SNR of a packet by using the SNR of the preamble. MoLoRa calculates the SNR of the preamble by leveraging dechirp results of the preamble in the frequency domain [23]. The calculated SNR serves as an indicator of real-time channel condition.

## 3.3 Searching for satisfactory state

*MoLoRa* starts receiving packets from a random initial state and then calculates SNR as an indicator of packet quality to decide whether the current state is optimal for packet receiving. The key challenge is how to search for the optimal state with high efficiency.

**Searching strategy.** Grid search and random search are two straightforward yet ineffective ways to find the best state. In grid search, we uniformly divide the reachable space into several states and test them one by one. The grid's granularity determines the number of tests and how closely we can approach the optimal state. For the robot arm prototype, the search space - a hemisphere with a radius of 1 m (*i.e.*, the length of robot arm) - consists of a 6-tuple configuration, where each 3D point allows for a 3-dimensional choice of roll, yaw, and pitch. Given the substantial search space (6D), it may require numerous attempts to discover the best state by using grid search. Random search encounters a similar predicament, struggling with the expansive search domain.

We aim to find the optimal state with fewer attempts. Because each attempt needs to explore a new state to receive a real-world packet, which may be received with better quality if we can find the optimal state earlier. Besides, the SNR may fall during the search process. Excessive explorations do not guarantee good packet reception.

MoLoRa leverages BayesOpt [16] to direct the search for optimal state with high efficiency. Unlike complex deep learning models, BayesOpt is well-suited for this scenario, where each test builds on prior outcomes. As wireless channels are continuous in space, the RSS or SNR at one location is spatially correlated with another, enabling MoLoRa to learn from previous exploration results and expedite the search process. Figure 6 (a) and (b) illustrate SNR spatial distribution in 3D from different angles of view. Figure 6 (c) shows the project of 3D SNR heatmap in table plane. This experiment is conducted with packets sent every 10 seconds in an indoor scenario.

The high-level objective of BayesOpt for our problem can be described as

$$x^* = \arg\max_{x \in \chi} f(x) \tag{4}$$

where $x$ is the state of an antenna (a 6-tuple consisting of position and orientation), $\chi$ is the reachable space of an antenna, and $f(x)$ is the unknown SNR distribution function. The basic idea of BayesOpt is to model the unknown objective function $f(x)$ as a probabilistic surrogate model, typically a Gaussian process (GP), and then use the acquisition function to iteratively select the next point to evaluate. In specific, the surrogate model fits the existing observed data points and quantifies the uncertainty of unobserved areas, while the acquisition function determines which areas in the domain of $f(x)$ are worth exploiting and what areas are worth exploring. The acquisition function gives a high value to areas where $f(x)$ is optimal or areas that it has not sampled at and vice versa. In

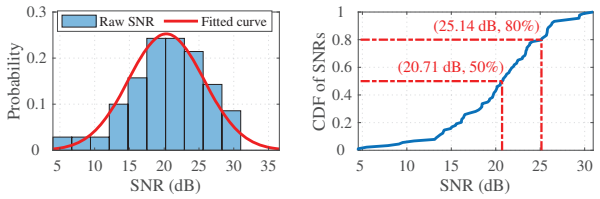


(a) Gaussian fitting of SNRs. (b) CDF of SNRs.

**Figure 7: Statistical analysis of SNR distribution.**

**Algorithm 1** BayesOpt for MoLoRa

**Require:** Target SNR gain $\Delta SNR_{th}$, Maximum attempt number $N$.
1: Initialization: randomly select a state $x_{t=0}$, get corresponding $SNR_{t=0}$, and form observation set $D_0 = \{x_{t=0}, SNR_{t=0}\}$.
2: **while** $(t \leq N)$ **do**
3: Find $x_t$ by optimizing the acquisition function over the GP: $x_t = \arg\max_x u(x|D_{1:t-1})$.
4: Move to $x_t$ and obtain $SNR_t$.
5: Augment observation set $D_{1:t} = \{D_{1:t-1}, (x_t, SNR_t)\}$ and update the GP.
6: **if** $SNR_t - SNR_{t-1} > \Delta SNR_{th}$ **then**
7: Break;
8: **end if**
9: **end while**
10: $x_t = \arg\max_x (x|D_{1:N})$ if cannot achieve target SNR gain in N attempts.

fact, instead of maximizing the unknown SNR distribution $f(x)$, BayesOpt maximizes the acquisition function. By finding $x$ that maximizes the acquisition function, BayesOpt identifies the next best guess of state for an antenna to receive a packet. In this setting, at iteration $n$, the antenna chooses a state $x_n$, at which to query $f$ (receive a LoRa packet) and evaluate $y = SNR_n$ as the result of $f(x_n)$. By iteratively updating the surrogate model and intelligently selecting the next state to evaluate, BayesOpt can efficiently explore the search space $\chi$ and is likely to reach a good state $x^*$ faster than the other two strawman solutions.

**Threshold setting.** Recall that our goal is to find an optimal state with fewer attempts. To obtain a proper threshold for BayesOpt termination condition, we investigate the distribution of SNRs in space. Specifically, we randomly collect 200 measurements of SNRs with different states and take the Shapiro-Wilk test [48]. Results show that we cannot reject the assumption that such data comes from a normally distributed population[1]. Figure 7 (a) and (b) show the Gaussian fitting and CDF of SNRs respectively. We can observe in Figure 7 (b) that though the achievable maximum SNR is more than 30 dB, 50% of the states have SNRs lower than 20.71 dB and 80% of the states have SNRs lower than 25.14 dB. In practice, it is impractical to measure as many as 200 states to search for an optimal state. And we cannot decide which state is the optimal state even with 200 samples. Besides, LoRa nodes have different SNR ranges when they are differently located. Therefore, we cannot set a fixed SNR threshold to determine whether a state is an optimal state or not.

Instead, we use SNR gain ($\Delta SNR$) as the threshold. Our intuition is that regardless of the receiving antenna's initial state, a larger SNR gain indicates a better search result. In practice, we note that the upper bound of SNR gain varies a lot with different initial states or among different nodes. As shown in Figure 7 (b), if the initial SNR is 15 dB, we may achieve as large as 15 dB SNR gain. However, if the initial state has an SNR of 25 dB, the achievable SNR gain is about 5 dB. Therefore, we set different levels of SNR gain thresholds (*e.g.*, 6 dB, 9 dB, and 12 dB) to adapt to different scenarios. A gateway can choose a 'satisfactory' SNR gain as its threshold to trade off between SNR gain and the number of attempts. We also set a maximum attempt number to avoid excessive exploration. If the receiver cannot meet the threshold within the maximum number of attempts, it will choose the state with the best SNR. Algorithm 1 summarizes this approach.

[1]We set the significance level to 0.05. The data has W = 0.9741 and $p$-value = 0.0675 .

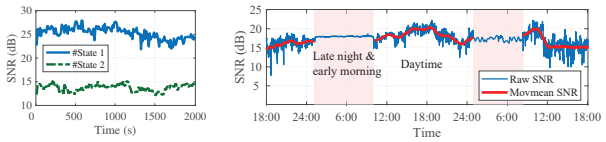


(a) T = 2000 s. (b) T = 2 days

**Figure 8: SNRs within (a) 2000 s and (b) 2 days.**

**Adaptive updating.** After a gateway finds an optimal state for receiving packets from a node, can this state be reused for subsequent packets from that node? We hope the wireless channel stays relatively stable so that a receiving antenna can identify an optimal state based on historical (both short-term and long-term) SNR records. To investigate LoRa channel stability in a practical network, we conduct experiments with packets sent every 10 seconds.

Figure 8 (a) shows the received SNR of two antenna states within a short period (2000 s). Although there are small variations, we observe that the SNRs of the two representative channels remain overall stable within a 2,000-second observation window. LoRa channel is relatively stable compared with other signals such as WiFi [25, 40]. However, as shown in Figure 8 (b), when stretching the time period to 2 days, we observe that though the SNRs are stable in late night and early morning, the variations are relatively large in busy daytime. Therefore, a receiver needs to re-search for a satisfactory state to adapt to environmental dynamics. Here we use SNR variation as a triggering condition. Empirically, when the measured SNR drops 6 dB for 3 consecutive packets, we will change the antenna states to adapt to the up-to-date conditions.

**Latency Issue.** LoRa's long-range, low-power design favors energy efficiency over high data rates. Thus, LoRa is not commonly used for real-time tasks due to its low data rate. MoLoRa's antenna switch delay is no more than 3 seconds and its design allows packet reception during switching, ensuring full compatibility with LoRa applications.

## 3.4 Extending to multiple nodes

So far, we have focused on improving the packet reception performance of a single node. In real-world, a LoRa gateway should support multiple nodes transmitting concurrently. Yet, it is time-consuming to change the states of a receiving antenna packet-by-packet. Moreover, due to the complex spatial distributions, an optimal Rx state for one node can be a blind spot for another node. It is challenging yet important to select a good receiving state that can improve the packet reception performance for multiple nodes simultaneously.

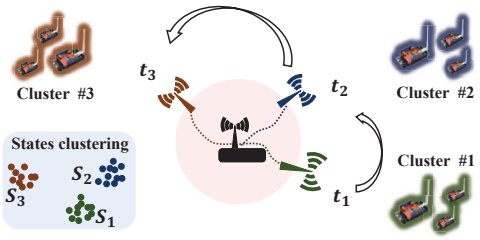


**Figure 9: Periodic reporting of multiple nodes.**

Although the optimal receiving states may vary across nodes due to differences in distances, locations, and physical channels, we observe that some nodes share close states in the search space. This indicates that it is possible to position a receiving antenna in a specific state to receive signals from multiple nodes, all with satisfactory performance. Note that a gateway in LoRaWAN uses beacon packets to provide a timing reference for Class B end devices [20]. Therefore, we group LoRa nodes into clusters and use beacons to schedule nodes in the same cluster to transmit concurrently, and their packets are received at a common antenna state. A MoLoRa gateway can decode these concurrent packets by incorporating SOTA parallel decoding methods like FTrack [74], making it possible for MoLoRa to scale well as the number of nodes increases. Nodes with contrasting SNR profiles (*e.g.*, nodes in good SNRs vs. nodes in bad SNRs) will be arranged into different clusters and scheduled with different antenna states. In this cluster-based approach, although the overall packet reception performance gain can be relatively lower compared to adapting the antenna state for each individual node, the antenna only needs to transit to one state for one cluster of nodes, thus avoiding frequent state changes.

MoLoRa groups nodes using K-means and employs the elbow method [24] to find the suitable number of clusters. We coordinate the data reporting of LoRa nodes according to their clusters and search for a common satisfactory state for nodes within a cluster by jointly optimizing the sum of SNR gain of that cluster. Specifically, the common receiving state of a cluster is initialized at the center of the optimal antenna states of all nodes in that cluster. A gateway then coordinates the transmission of nodes in this cluster and calculates the total SNR gain. The gateway adds empirical shifts to the central state and repeats above process three times. The state with the highest total SNR gain is selected as the optimal state for that cluster. As shown in Figure 9, a gateway allocates different periodic transmission slots for nodes in different clusters and the mobile antenna changes its state periodically to receive packets from different groups. The coordination overhead increases with the number of clusters, but this also enhances overall SNR gain. Practical implementation requires balancing these trade-offs.

**Compatibility with LoRaWAN standards.** The above design focuses on enabling multi-packet reception from Class B nodes, where packet transmission can be coordinated by using beacons, as demonstrated in previous work [20] for data aggregation applications. Since the duty cycle of LoRa transmission is no more than 1%, an antenna usually has adequate time to transit to a new target state for incoming packets. Empirically, we reserve 3 seconds for state transition. However, Class A and C devices in LoRa networks send uplink packets randomly to a gateway, making it impractical for a receiving antenna to transition to an optimal state in time for each randomly arriving packet. Although MoLoRa may not consistently achieve an optimal antenna state for every packet from these devices, it can leverage historical exploration data to select a position and orientation that statistically maximizes reception quality for the majority of nodes. This approach minimizes the likelihood of blind spots by avoiding positions that historically result in poor reception. By prioritizing states with a higher probability of successful packet reception, MoLoRa enhances coverage and maintains robust reception across the network, even under the non-coordinated transmission patterns of Class A and C devices. Performance of MoLoRa with different types of ended nodes can be found in Sec. 4.3.

**Energy cost of MoLoRa.** Gateways are typically deployed with tethered power supplies, making the additional energy required for antenna movement manageable. For end nodes, Class A and Class C devices operate as usual as with a standard commodity gateway, incurring no extra energy cost for the SNR gains achieved. Class B devices are required to periodically receive beacons and open ping slots to obtain timing references and coordination messages in standard LoRaWAN. With these timing references, the network server can schedule downlinks to specific devices or groups of devices [60]. MoLoRa embeds minimal coordination information (a few bytes) into these downlink messages during ping slots. Consequently, Class B nodes in MoLoRa expend only slightly more energy to receive this additional coordination data—an increase that is negligible compared to their standard energy usage. Critically, Regardless of device type, LoRa nodes in blind spots continuously transmit uplinks, rapidly draining their batteries. Traditional methods like XCopy exacerbate this issue by requiring multiple retransmissions to improve SNR, significantly increasing energy consumption. In contrast, MoLoRa enhances packet reception efficiency, reducing retransmissions and substantially extending battery life—making it a highly energy-efficient solution for battery-powered LoRa nodes.

Note that MoLoRa focuses on predicting optimal state for packet reception with high efficiency. It does not consider the joining/roaming process of nodes to/between multiple gateways and the changing of clusters over a long time at the current design stage. We leave these for future research.

# 4 IMPLEMENTATION AND EVALUATION

## 4.1 Implementation

**Hardware.** MoLoRa can be implemented with any actuation devices that can change the position and orientation of an antenna. Here we first present an advanced version as a proof-of-concept. Specifically, we use a high-end robot arm JAKA Zu 3 [26] with six degrees of freedom (6-DOF) to change the antenna state. We use VERT900 [46] as a receiving antenna and mount it to the gripper of the robot arm. The antenna is connected to USRP N210 via coaxial cables. Here we use USRP for convenient access to raw data and algorithm testing. Corresponding algorithms can be integrated into a COTS gateway for future implementation. A laptop (Intel Core i9-13980HX @ 2.2GHz) is used as an edge server to run the state search algorithm and control the robot arm. We also implement low-cost and low-DoF devices (*e.g.*, sliding tracks and gimbals) to

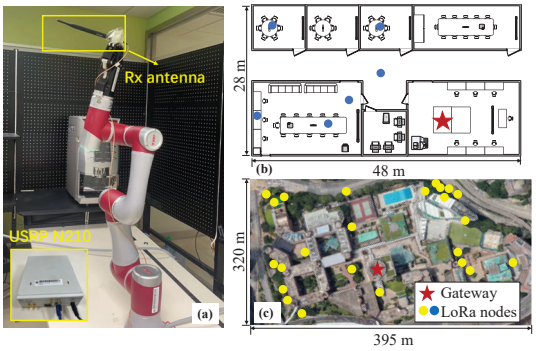


**Figure 10: (a) Advanced prototype of MoLoRa (b) indoor and (c) outdoor experiment layout.**

build dimensionality-reductioned prototypes of mobile antenna systems in §4.3.7 for ablation study. In practice, developers can choose suitable moving devices according to their budgets and needs.

**Software.** We integrate data pre-processing described in §3.2 into an open-source project of LoRa implementation `gr-lora` [19], and transmit the processing result (*i.e.*, packet SNR) to the edge server through socket communication. The server runs BayesOpt-based search algorithm and sends commands (*i.e.*, next state) to the robot arm through Wi-Fi communication. Our code is developed in Python and C++. MoLoRa achieves real-time packet data processing and control of the robot arm. We also process packets offline in MATLAB for performance comparison.

## 4.2 Evaluation methodology

**Experiment setup.** MoLoRa is tested with COTS LoRa nodes (LoRa Shield). Figure 10 (b) and (c) show our testbed, which consists of 30 LoRa nodes and a mobile receiver. We place LoRa nodes in rooms inside buildings and outside areas across our campus. For the convenience of experiments, we locate the mobile antenna inside a lab room. We configure all nodes to work at 915 MHz ISM band and set the default transmission power to 20 dBm. We also configure all nodes to work in an ADR mode, with which nodes properly choose a spreading factor according to the SNRs of underlying wireless links. The gateway sends beacon signals to coordinate the transmission of LoRa nodes. After receiving all packets from one cluster, the mobile antenna changes its state to receive packets from another cluster. In our experiment, 30 nodes are divided into 3 clusters, depending on their SNR profiles, and more than 10,500 packets are transmitted for over four months to evaluate MoLoRa. These packets can cover diverse channel conditions in typical urban scenarios (*e.g.*, blockages, multipath, dynamic traffic, *etc.*)

**Comparison.** MoLoRa uses *BayesOpt* to search antenna states for achieving a certain SNR gain. We compare MoLoRa against (1) a *Baseline* receiver with a fixed antenna state, moving antennas with (2) *Random search* and (3) *Grid search*, and (4) a SOTA method *XCopy* [72].

**Metrics.** We evaluate MoLoRa with various metrics: (1) *SNR of packets*; (2) *Symbol Error Rate (SER)* of packet decoding; (3) *Packet Reception Ratio (PRR)* of link communication; (4) *Throughput* of a communication link. These metrics characterize the signal quality and communication performance of MoLoRa. We also use (5) *Number of attempts* to evaluate the efficiency of MoLoRa in terms of how many rounds of searches are required to achieve a target SNR gain.

## 4.3 Evaluation results

*4.3.1 Basic performance.* **Packet reception performance improvement.** In this experiment, we evaluate the packet reception performance of MoLoRa. We first collect packets from 30 LoRa nodes with a fixed antenna. We collect 30 packets from each node. For fairness, we randomly choose 5 states within the search space of a robot arm and use the average results as the performance of a fixed antenna (baseline). We then receive packets with a moving antenna. For each node, we try at most 15 states using BayesOpt. We collect 30 packets at satisfactory states and calculate the corresponding packet reception performance.

Figure 11 presents a comparison of communication performance between a fixed antenna and MoLoRa. Specifically, Figure 11(a) illustrates the average SNRs of packets received by these two methods. We observe that MoLoRa achieves an average SNR that is 7 dB higher than that of the fixed-state antenna. Notably, the average SNR of the first node is −10.6 dB when received by the fixed antenna, with the lowest received SNR dropping to −15 dB – indicating that this node may be in a blind spot. In contrast, by employing a mobile receiving antenna, the average SNR increases to 1.4 dB. This example demonstrates that MoLoRa can effectively help a node in a blind spot to reconnect to the network.

Figure 11 (b) shows the average symbol error rate (SER) of these two methods. We see that MoLoRa achieves nearly 0 SER for all nodes in the network while the average SER of the baseline is as high as around 0.3. Besides, the SER standard deviation of the baseline is much higher than that of MoLoRa. This result demonstrates that the communication performance of a fixed antenna highly depends on the state it chooses. MoLoRa empowers mobility to the antenna to search for a good receiving state and avoid those bad states. Figure 11 (c) presents the corresponding packet reception rate (PRR). Results show that a fixed antenna can only receive no more than 65% of the packets. In contrast, a mobile antenna achieves a packet reception rate of 100%.

We further evaluate the throughput of the network. As shown in Figure 11 (d), the throughput first increases as the number of nodes increases and then keeps rather static when the number of nodes exceeds 10. In fact, the turning point should be 8 due to the gateway's parallel decoding capability. As expected, a mobile antenna performs much better than a fixed one. Specifically, MoLoRa achieves an average throughput of 6 kbps when there are more than 10 nodes in the network while a fixed antenna can only achieve around 4 kbps. MoLoRa boosts 50% throughput for LoRaWAN in urban settings. The above experiment results demonstrate that empowering receiving antenna with motion can greatly improve the packet reception performance of LoRaWANs.

*4.3.2 Comparison with state-of-the-art.* We compare MoLoRa with the state-of-the-art method XCopy [72], which combines multiple re-transmitted packets to improve weak packet reception, to evaluate their performance in low-SNR scenarios. For fairness, we keep other transmission settings the same, control the packet SNR to be

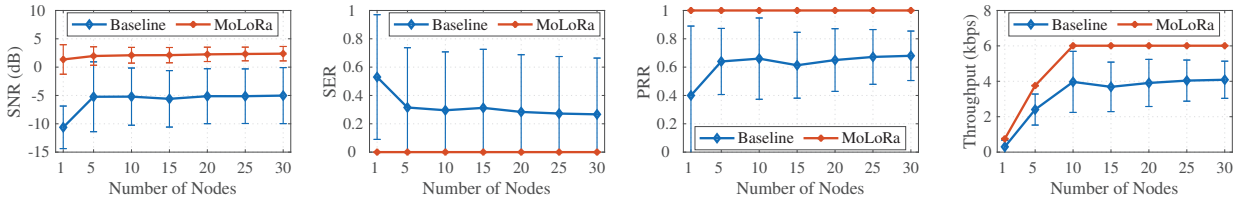


(a) SNR (b) SER (c) PRR (d) Throughput

**Figure 11: Packet reception improvement.**

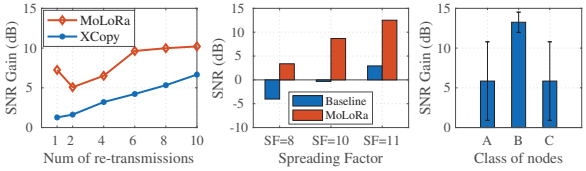


**Figure 12: MoLoRa vs XCopy.**

**Figure 13: ADR compatibility.**

**Figure 14: Node classes.**

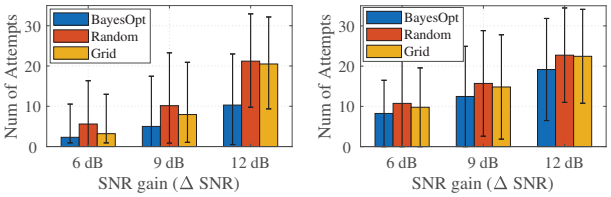


(a) Initial state with low-SNR (b) Random initial state

**Figure 15: Number of attempts to reach target SNR gain.**

−20 dB, and let a LoRa node re-transmit the same packet 10 times. We use a fixed antenna to receive packets for XCopy; whereas allowing antenna movements to an optimal state for MoLoRa. The fixed and mobile antenna can be regarded as co-located considering the long transmission range of LoRa.

Figure 12 displays the SNR gain comparison with different numbers of re-transmissions. MoLoRa produces 4 dB higher SNR gains than XCopy with the same number of re-transmissions/attempts. MoLoRa only needs 4 attempts to achieve 6 dB SNR gain, whereas XCopy requires 10 re-transmissions to achieve a comparable performance. It is noteworthy that MoLoRa's SNR gain fluctuates during the first few attempts, while XCopy's SNR gain increases almost linearly as the number of re-transmissions increases. In fact, MoLoRa and XCopy are complementary strategies that can be used together to improve communication performance in challenging channel conditions.

*4.3.3 Compatibility with ADR.* This experiment evaluates the compatibility of MoLoRa with LoRaWAN's ADR scheme. In this experiment, we adjust SF to represent ADR as this is the core technology in ADR scheme. We put a LoRa node at a none-line-of-sight position 200 m away from two co-located receivers: a baseline receiver running ADR with a fixed antenna and a MoLoRa receiver running ADR as well as BayesOpt. We set SF to 8 at the beginning of experiments and gradually increased SF to 10 and 11. We collect 30 packets for each SF and calculate the average SNR.

Figure 13 presents the SNR under different SFs. As ADR increases SF, both baseline method and MoLoRa receive packets with higher SNRs. The average SNR gain achieved by ADR increasing SF by one is 2.32 dB for the fixed antenna. MoLoRa achieves an average of 8.66 dB higher SNR than the baseline under the same SF setting due to the mobility of the antenna. This experiment demonstrates that MoLoRa can jointly work with ADR for better performance.

*4.3.4 Performance across different classes of nodes.* In this experiment, we evaluate MoLoRa's performance across different classes of LoRa nodes. We deploy a testbed of 30 LoRa nodes, sequentially configuring them as Class A, B,C to assess MoLoRa's performance with each. For the Class B configuration, we apply the same setup stated in §4.2. In the Class A and C cases, MoLoRa first explores the available state space, then selects the optimal state with the highest probability of achieving robust reception across all nodes. We set the number of attempts to 30 and collect over 150 packets per class to calculate the resulting SNR gain in each scenario.

Figure 14 shows MoLoRa's SNR gain across different node classes. Class B nodes achieve the highest average SNR gain at 13 dB, while Class A and C nodes achieve lower gains, averaging no more than 6 dB. Additionally, the SNR gain in Class A and C nodes shows a higher standard deviation compared to Class B nodes. This is expected, as MoLoRa identifies optimal receiving states with finer granularity (in terms of the number of nodes) for Class B nodes due to their working patterns capable of supporting periodic transmission.

*4.3.5 Search efficiency.* **Searching strategy comparison.** We compare BayesOpt search with random search and grid search and evaluate the number of attempts to achieve a target SNR gain. Considering that different initial states may have an impact on the number of attempts, we conduct two experiments with different initial states of nodes. In the first experiment, we select 10 nodes with low PRR (<70%) and SNR (<-15 dB) in non-line-of-sight scenarios when using a fixed antenna. These nodes are likely to fall into blind spots. In the second experiment, we randomly select 10 nodes in the network, aiming to cover different kinds of channel conditions. We configure the maximum attempt number to 30. We mark 31 attempts if the antenna cannot achieve the target SNR gain within 30 attempts.

Figure 15 shows the number of attempts required to achieve target SNR gains in two experiments. By comparing the results, we observe that for nodes with poor initial conditions, all three

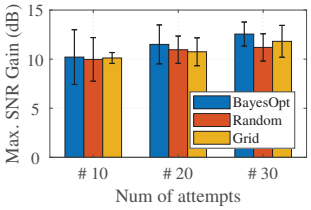


**Figure 16: Maximum SNR gain.**

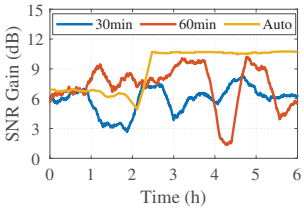


**Figure 17: Update methods.**

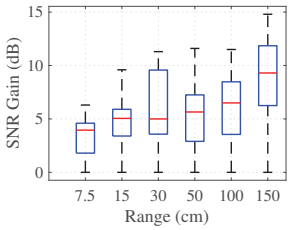


**Figure 18: MoLoRa's SNR gain as a function of the available area to change the antenna's states.**

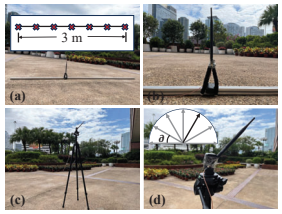


**Figure 19: (a) and (b): benchmarking with slide track; (c) and (d): benchmarking with gimbal.**

searching strategies achieve the target SNR gains with relatively few explorations. Specifically, BayesOpt achieves 6 dB SNR gain with an average of 2.3 search attempts when the initial state is low-SNR, whereas it requires 8.24 search attempts to achieve the same gain with a random initial state. These results indicate that a mobile antenna is efficient at improving the link quality of nodes in suboptimal conditions (e.g., non-line-of-sight, multipath environments). Regarding the searching efficiency of different strategies, BayesOpt outperforms both grid search and random search in both experiments. For example, in Figure 15(a), BayesOpt achieves a 12 dB SNR gain with an average of 10.3 attempts, whereas random and grid search require 21.2 and 20.5 attempts, respectively—both approximately twice the number of attempts needed by BayesOpt. Additionally, we observe that, on average, achieving higher SNR gains necessitates more explorations. In practice, users must set appropriate target SNR gains to balance the cost of explorations.

**Maximum SNR gain comparison.** We also evaluate the maximum SNR gains and plot results in Figure 16. We find that all three methods can achieve a maximum SNR gain of 10 to 13 dB with a sufficient number of attempts ($\geq 10$). Among these methods, BayesOpt achieves the highest maximum SNR gain, followed by Grid search. As the number of attempts increases, the SNR gains increase, and the advantage of BayesOpt and Grid search increases. This improvement is likely because the surrogate model used in Bayesian optimization and the granularity of Grid search increasingly approximate the true distribution of the signal in space as the number of sampling points grows. Consequently, BayesOpt can approach the optimal receiving state with more precise parameters than the other two methods.

**Impact of updating methods.** Next, we evaluate the impact of channel dynamics and the benefit of our adaptive updating methods. In this experiment, we transmit packets every 10 seconds and implement 3 updating strategies that search for satisfactory states every 30 min, 60 min, and automatically update upon detecting 3 consecutive packets with 6 dB gain loss. Figure 17 plots the results of SNR gains of these three methods for 6 hours. We observe that in the first hour, three methods achieve similar SNR gain. In the second hour, the per-hour updating method achieves the best performance, followed by the auto-updating method. This may be attributed to the antenna maintaining a static state, as there is no consecutive 6 dB SNR loss during this period. In contrast, our adaptive updating method outperforms the other two interval updating methods in the last 4 hours. We infer that the channel condition has changed greatly from 3.5-4.5 h, resulting in a severe drop of SNR gains for the per-hour updating method since it cannot adapt to changes timely. By contrast, our automated state-searching method can keep tracking the optimal state to combat channel dynamics.

*4.3.6 Microbenchmarking of movable area.* This experiment evaluates MoLoRa's performance across different state changing areas. We gradually increase the radius of the state-changing space from 7.5 cm to 150 cm, receiving 30 packets at random antenna states within each radius. For each radius, we calculate the SNR gain by using the packet with the minimum SNR as the reference point.

As shown in Figure 18: when the state-changing space expands, the average SNR gain improves significantly. Specifically, MoLoRa achieves an average SNR gain of 5 dB within a 30 cm movable area. When the range is extended to 150 cm, the average SNR gain increases to about 10 dB, indicating that movable range is one influencing factor of MoLoRa. These results demonstrate that enabling antenna mobility within just 0.1% to 1% of the LoRa communication range yields substantial SNR gains, highlighting MoLoRa's effectiveness in utilizing small-scale movement to enhance LoRa packet reception.

*4.3.7 Microbenchmarking with low-cost and easy-to-setup actuation devices.* In the previous experiments, we change the state of antenna with high-end robot arm. Here we use low-end actuation machines to narrow the search space to 1-DoF and benchmark the gain of micro-mobility. Specifically, we conduct experiments with a slide track ($10 USD) and a gimbal ($22 USD), which are low-cost and easy to set up.

As shown in Figure 19, we select 7 points on a 3 m-long track to receive LoRa packets. These points are equally spaced with an interval of 0.5 m. A LoRa node is placed 50 m away from the receiver with no line-of-sight path. The LoRa node is configured to transmit every 1 second. We collect 15 packets at each state and move to the next. Similarly, for the experiment with a gimbal, we select 7 receiving angles $\alpha$ (the angle between the antenna and the left side of a horizontal line) by adjusting the shift angle of the gimbal. In this experiment, we only change the roll of the antenna in a step of $30^\circ$, ensuring that the antenna is positioned with different receiving angles in the same plane.

**Performance with slide track.** Figure 20 shows the measured SNRs of packets received at different positions of a slide track. We can observe that the receiving antenna has the lowest SNR of 9.4 dB when it is positioned at the left start point of the track. As the antenna moves from left to right, the average SNR increases, but there is a slight decrease at the right endpoint. The gateway achieves

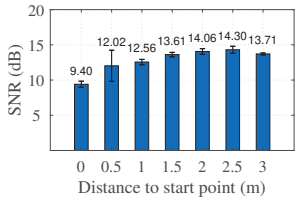


**Figure 20: Slide track result.**

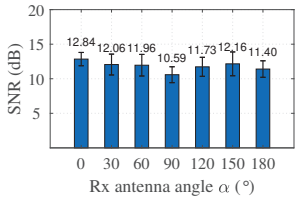


**Figure 21: Gimbal result.**

its highest average SNR of 14.3 dB when the antenna is positioned 2.5 m away from the left starting point. In this experiment, the overall SNR gain of micro-mobility in one dimension is 2.9 dB. The result demonstrates that low-cost and low-DoF devices such as a slide track can also be effective in enhancing LoRa reception performance. Besides, this experiment demonstrates the feasibility of employing a mobile antenna to measure the instantaneous channel condition.

**Performance with gimbal.** Figure 21 reports the channel condition measured by different receiving angles within a plane. It can be observed that the average SNRs vary across different angles. The SNR gain by adjusting the roll of the receiving antenna with a gimbal is 2.25 dB. To our surprise, the antenna achieves the worst SNR of 10.59 dB when the antenna angle $\alpha$ is 90°, where the transmitting antenna and receiving antenna are physically aligned. In contrast, it achieves the highest SNR of 12.84 dB when the antenna angle $\alpha$ is 0°, where the transmitting antenna and receiving antenna are orthogonally positioned. This result indicates that the angle of the transmitted signal's electrical magnetic (EM) has been twisted 90° by the environment before it arrives at the receiver. This experiment again demonstrates that even 1-DoF mobility brought by a simple actuation device can improve the packet reception performance of LoRa.

**Future design of actuators.** Previous experiments have proved MoLoRa's feasibility on low-cost actuators, even with only 1-DoF mobility. MoLoRa's gain increases when provided with more degrees of freedom. In the future, we consider exploring programmable antenna technique [3] at the gateway of MoLoRa to replace real-world mechanical movement and save cost.

## 5 RELATED WORK

Many studies [1, 11, 12, 17, 21, 34, 41, 42, 55, 62, 65, 67, 72, 73, 75, 77, 80] have aimed to enhance the communication reliability of LoRa. Charm [8] collaborates multiple gateways to improve link quality. Falcon [63] allows weak links to selectively interfere with ongoing transmissions to extend LoRa coverage. MALoRa [23] coherently combines signal copies from synchronized antennas to receive weak LoRa packets. These works either require complex hardware with high cost or sacrifice data rate. NELoRa [33] uses neural networks at the gateway to enhance weak packets. However, it trains various networks for packets with different parameters. By contrast, MoLoRa empowers intelligence and mobility to Rx antenna to boost packet reception in a lightweight manner. MoLoRa also complements ADR of LoRaWAN.

**Intelligent hardware in wireless network.** Many studies have demonstrated the benefits of intelligent hardware for wireless communication [69, 76]. Some works use mobile access points [86] and relays to enhance network performance for WiFi [6], RFID [43], and mmWave [85]. Recent advances in smart surface [13, 14, 47] reshape beamforming to illuminate blind spots and increase link capacity. Unlike these works, MoLoRa is specifically designed for LoRaWAN to detect ultra-weak packets and combat blockage and small-scale fading. MoLoRa designs and implements an intelligent mobile antenna that can automatically adjust antenna position and orientation for incoming LoRa packets.

**Antenna polarization in LoRa.** Antenna polarization poses a challenge for mobile LoRa devices, as it leads to unstable link quality, blind spots, and further degrades network performance. PolarTracker [70] introduces an orientation-aware channel access method that adapts to the antenna polarization. PolarScheduler [36] further proposes a dynamic transmission control method that optimizes the transmission configuration to improve both reliability and throughput. Demeter [53] leverages programmable polarization with additional hardware at end nodes to improve link quality. Unlike previous works, MoLoRa enables mobile Rx antenna to actively adjust for the best-polarized directivity without incurring costs at low-end nodes.

## 6 CONCLUSION

In this paper, we present the design and implementation of MoLoRa, an intelligent mobile antenna system that automatically searches for optimal positions and orientations for enhanced LoRa packet reception. MoLoRa puts together a series of novel techniques for detecting packets, searching for satisfactory states, and joint optimization for multiple packets. MoLoRa provides a new perspective on the challenging problems in LoRa networking such as blind spots and line-of-sight path blockages. Experiments show that MoLoRa can potentially improve SNR by 13 dB. Moreover, by dynamically adjusting the receiving antenna, MoLoRa can effectively create new paths and cover those nodes in blind spots that would otherwise never be saved with existing solutions like packet retransmissions or power adaptation.

## ACKNOWLEDGEMENTS

We sincerely appreciate the valuable comments and feedback from the anonymous shepherd and reviewers. This work is supported in part by the Macquarie University Research Acceleration Scheme and in part by the Hong Kong General Research Fund (GRF) under grants 15211924, 15206123, 15218022, and 15231424. Yuanqing Zheng and Tao Gu are the corresponding authors.

## REFERENCES

[1] Absar-Ul-Haque Ahmar, Emekcan Aras, Thien Duc Nguyen, Sam Michiels, Wouter Joosen, and Danny Hughes. 2023. Design of a Robust MAC Protocol for LoRa. *ACM Trans. Internet Things* 4, 1, Article 3 (feb 2023), 25 pages. https://doi.org/10.1145/3557048

[2] Constantine A Balanis. 2016. *Antenna theory: analysis and design.* John wiley & sons.

[3] Dingzhao Chen, Yanhui Liu, Ming Li, Pan Guo, Zhuo Zeng, Jun Hu, and Y Jay Guo. 2022. A polarization programmable antenna array. *Engineering* 16 (2022), 100–114.

[4] Yuning Chen, Kang Yang, Zhiyu An, Brady Holder, Luke Paloutzian, Khaled Bali, and Wan Du. 2024. MARLP: Time-series Forecasting Control for Agricultural Managed Aquifer Recharge. In *Proceedings of the 30th ACM SIGKDD Conference on Knowledge Discovery and Data Mining (KDD'24).*

[5] Kaiyan Cui, Qiang Yang, Leming Shen, Yuanqing Zheng, Fu Xiao, and Jinsong Han. 2024. Towards ISAC-Empowered mmWave Radars by Capturing Modulated

Vibrations. *IEEE Transactions on Mobile Computing* (2024).
[6] Ashutosh Dhekne, Mahanth Gowda, Romit Roy Choudhury, and Srihari Nelakuditi. 2018. If WiFi APs Could Move: A Measurement Study. *IEEE Transactions on Mobile Computing* 17, 10 (2018), 2293–2306. https://doi.org/10.1109/TMC.2018.2799933
[7] DJI. 2023. *DJI RS3 Gimbal Combo.* https://www.jbhifi.com.au/products/dji-rs3-gimbal-combo
[8] Adwait Dongare, Revathy Narayanan, Akshay Gadre, Anh Luong, Artur Balanuta, Swarun Kumar, Bob Iannucci, and Anthony Rowe. 2018. Charm: exploiting geographical diversity through coherent combining in low-power wide-area networks. In *2018 17th ACM/IEEE International Conference on Information Processing in Sensor Networks (IPSN)*. IEEE, 60–71.
[9] Dragino. 2021. *LoRa Shield for Arduino.* Retrieved Mar 25, 2021 from http://www.dragino.com/products/module/item/102-lora-shield.html
[10] Jialuo Du, Yunhao Liu, Yidong Ren, Li Liu, and Zhichao Cao. 2024. LoRaTrimmer: Optimal Energy Condensation with Chirp Trimming for LoRa Weak Signal Decoding. In *Proceedings of the 30th Annual International Conference on Mobile Computing and Networking*.
[11] Jialuo Du, Yidong Ren, Mi Zhang, Yunhao Liu, and Zhichao Cao. 2023. NELoRa-Bench: A Benchmark for Neural-enhanced LoRa Demodulation. *arXiv preprint arXiv:2305.01573* (2023).
[12] Jialuo Du, Yidong Ren, Zhui Zhu, Chenning Li, Zhichao Cao, Qiang Ma, and Yunhao Liu. 2023. SRLoRa: Neural-enhanced LoRa Weak Signal Decoding with Multi-gateway Super Resolution. In *Proceedings of the Twenty-fourth International Symposium on Theory, Algorithmic Foundations, and Protocol Design for Mobile Networks and Mobile Computing*. 270–279.
[13] Manideep Dunna, Chi Zhang, Daniel Sievenpiper, and Dinesh Bharadia. 2020. ScatterMIMO: Enabling virtual MIMO with smart surfaces. In *Proceedings of the 26th Annual International Conference on Mobile Computing and Networking*. 1–14.
[14] Chao Feng, Xinyi Li, Yangfan Zhang, Xiaojing Wang, Liqiong Chang, Fuwei Wang, Xinyu Zhang, and Xiaojiang Chen. 2021. RFlens: metasurface-enabled beamforming for IoT communication and sensing. In *Proceedings of the 27th Annual International Conference on Mobile Computing and Networking*. 587–600.
[15] Ana Elisa Ferreira, Fernando M Ortiz, Luis Henrique MK Costa, Brandon Foubert, Ibrahim Amadou, and Nathalie Mitton. 2020. A study of the LoRa signal propagation in forest, urban, and suburban environments. *Annals of Telecommunications* 75 (2020), 333–351.
[16] Peter I Frazier. 2018. A tutorial on Bayesian optimization. *arXiv preprint arXiv:1807.02811* (2018).
[17] Akshay Gadre, Revathy Narayanan, Anh Luong, Anthony Rowe, Bob Iannucci, and Swarun Kumar. 2020. Frequency Configuration for Low-Power Wide-Area Networks in a Heartbeat.. In *NSDI*. 339–352.
[18] Amalinda Gamage, Jansen Liando, Chaojie Gu, Rui Tan, Mo Li, and Olivier Seller. 2023. LMAC: Efficient carrier-sense multiple access for LoRa. *ACM Transactions on Sensor Networks* 19, 2 (2023), 1–27.
[19] Gr-LoRa GitHub community. 2021. *gr-lora projects.* Retrieved Mar 15, 2021 from https://github.com/rpp0/gr-lora
[20] Ningning Hou, Xianjin Xia, Yifeng Wang, and Yuanqing Zheng. 2024. One shot for all: Quick and accurate data aggregation for LPWANs. *IEEE/ACM Transactions on Networking* (2024).
[21] Ningning Hou, Xianjin Xia, and Yuanqing Zheng. 2021. Jamming of LoRa PHY and Countermeasure. In *IEEE INFOCOM 2021-IEEE Conference on Computer Communications*. IEEE, 1–10.
[22] Ningning Hou, Xianjin Xia, and Yuanqing Zheng. 2022. Cloaklora: A covert channel over lora phy. *IEEE/ACM Transactions on Networking* 31, 3 (2022), 1159–1172.
[23] Ningning Hou, Xianjin Xia, and Yuanqing Zheng. 2023. Don't miss weak packets: Boosting LoRa reception with antenna diversities. *ACM Transactions on Sensor Networks* 19, 2 (2023), 1–25.
[24] Hestry Humaira and R Rasyidah. 2020. Determining the appropiate cluster number using Elbow method for K-Means algorithm. In *Proceedings of the 2nd Workshop on Multidisciplinary and Applications (WMA) 2018, 24-25 January 2018, Padang, Indonesia.*
[25] Bashima Islam, Md Tamzeed Islam, Jasleen Kaur, and Shahriar Nirjon. 2019. Lorain: Making a case for lora in indoor localization. In *2019 IEEE international conference on pervasive computing and communications workshops (PerCom workshops)*. IEEE, 423–426.
[26] JAKA Robotics . 2023. *JAKA Zu 3.* https://www.jakarobotics.com/products/jaka-zu/zu-3/
[27] JEM Engineering. 2020. *Intro to Antenna Polarization.* Retrieved Jul 2023 from https://jemengineering.com/blog-intro-to-antenna-polarization/
[28] Jinyan Jiang, Jiliang Wang, Yijie Chen, Yihao Liu, and Yunhao Liu. 2023. Locra: Enable practical long-range backscatter localization for low-cost tags. In *Proceedings of the 21st Annual International Conference on Mobile Systems, Applications and Services*. 317–329.
[29] Jinyan Jiang, Jiliang Wang, Yijie Chen, Shuai Tong, Pengjin Xie, Yihao Liu, and Yunhao Liu. 2024. Willow: Practical WiFi Backscatter Localization with Parallel Tags. In *Proceedings of the 22nd Annual International Conference on Mobile Systems, Applications and Services*. 265–277.
[30] Jinyan Jiang, Jiliang Wang, Yihao Liu, Yijie Chen, and Yunhao Liu. 2024. WiCloak: Protect Location Privacy of WiFi Devices. In *2024 23rd ACM/IEEE International Conference on Information Processing in Sensor Networks (IPSN)*. IEEE, 101–112.
[31] Jinyan Jiang, Zhenqiang Xu, Fan Dang, and Jiliang Wang. 2021. Long-range ambient LoRa backscatter with parallel decoding. In *Proceedings of the 27th Annual International Conference on Mobile Computing and Networking*. 684–696.
[32] Lieve Lauwers, Kurt Barbé, Wendy Van Moer, and Rik Pintelon. 2009. Estimating the parameters of a Rice distribution: A Bayesian approach. In *2009 IEEE Instrumentation and Measurement Technology Conference*. IEEE, 114–117.
[33] Chenning Li, Hanqing Guo, Shuai Tong, Xiao Zeng, Zhichao Cao, Mi Zhang, Qiben Yan, Li Xiao, Jiliang Wang, and Yunhao Liu. 2021. NELoRa: Towards Ultra-Low SNR LoRa Communication with Neural-Enhanced Demodulation. In *Proceedings of the 19th ACM Conference on Embedded Networked Sensor Systems* (Coimbra, Portugal) *(SenSys '21)*. Association for Computing Machinery, New York, NY, USA, 56–68. https://doi.org/10.1145/3485730.3485928
[34] Chenning Li, Yidong Ren, Shuai Tong, Shakhrul Iman Siam, Mi Zhang, Jiliang Wang, Yunhao Liu, and Zhichao Cao. 2024. ChirpTransformer: Versatile LoRa Encoding for Low-power Wide-area IoT. In *Proceedings of the 22nd Annual International Conference on Mobile Systems, Applications and Services*. 479–491.
[35] Ruonan Li, Ziyue Zhang, Xianjin Xia, Ningning Hou, Wenchang Chai, Shiming Yu, Yuanqing Zheng, and Tao Gu. 2025. From Interference Mitigation to Toleration: Pathway to Practical Spatial Reuse in LPWANs. In *in Proc. of ACM MobiCom 2025*.
[36] Ruinan Li, Xiaolong Zheng, Yuting Wang, Liang Liu, and Huadong Ma. 2022. PolarScheduler: Dynamic Transmission Control for Floating LoRa Networks. In *IEEE INFOCOM 2022 - IEEE Conference on Computer Communications*. 550–559. https://doi.org/10.1109/INFOCOM48880.2022.9796656
[37] Jansen C Liando, Amalinda Gamage, Agustinus W Tengourtius, and Mo Li. 2019. Known and unknown facts of LoRa: Experiences from a large-scale measurement study. *ACM Transactions on Sensor Networks (TOSN)* 15, 2 (2019), 1–35.
[38] Daniel Bonilla Licea, Mounir Ghogho, Des McLernon, and Syed AR Zaidi. 2019. Antenna controller for low-latency and high reliability robotic communications over time-varying fading channels. In *2019 27th European Signal Processing Conference (EUSIPCO)*. IEEE, 1–5.
[39] Yicheng Lin, Wei Yu, and Yves Lostanlen. 2012. Optimization of wireless access point placement in realistic urban heterogeneous networks. In *2012 IEEE Global Communications Conference (GLOBECOM)*. IEEE, 4963–4968.
[40] Jun Liu, Jiayao Gao, Sanjay Jha, and Wen Hu. 2021. Seirios: leveraging multiple channels for LoRaWAN indoor and outdoor localization. In *Proceedings of the 27th Annual International Conference on Mobile Computing and Networking*. 656–669.
[41] Jun Liu, Weitao Xu, Sanjay Jha, and Wen Hu. 2020. Nephalai: towards LPWAN C-RAN with physical layer compression. In *Proceedings of the 26th Annual International Conference on Mobile Computing and Networking*. 1–12.
[42] Junzhou Luo, Zhuqing Xu, Jingkai Lin, Ciyuan Chen, and Runqun Xiong. 2023. CH-MAC: Achieving Low-latency Reliable Communication via Coding and Hopping in LPWAN. *ACM Trans. Internet Things* 4, 4, Article 24 (nov 2023), 25 pages.
[43] Yunfei Ma, Nicholas Selby, and Fadel Adib. 2017. Drone relays for battery-free networks. In *Proceedings of the Conference of the ACM Special Interest Group on Data Communication*. 335–347.
[44] Qianhe Meng, Han Wang, Chong Zhang, Yihang Song, Songfan Li, Li Lu, and Hongzi Zhu. 2024. Processor-Sharing Internet of Things Architecture for Large-scale Deployment. In *Proceedings of the 22nd ACM Conference on Embedded Networked Sensor Systems*. 211–224.
[45] Luca Mottola, Thiemo Voigt, and Gian Pietro Picco. 2013. Electronically-switched directional antennas for wireless sensor networks: A full-stack evaluation. In *2013 IEEE International Conference on Sensing, Communications and Networking (SECON)*. IEEE, 176–184.
[46] NI. 2020. *VERT900 Antenna.* Retrieved Aug 14, 2020 from https://www.ettus.com/all-products/vert900/
[47] Kun Qian, Lulu Yao, Xinyu Zhang, and Tse Nga Ng. 2022. MilliMirror: 3D printed reflecting surface for millimeter-wave coverage expansion. In *Proceedings of the 28th Annual International Conference on Mobile Computing And Networking*. 15–28.
[48] Nornadiah Mohd Razali, Yap Bee Wah, et al. 2011. Power comparisons of shapiro-wilk, kolmogorov-smirnov, lilliefors and anderson-darling tests. *Journal of statistical modeling and analytics* 2, 1 (2011), 21–33.
[49] Kate A Remley, William Frederick Young, and Jacob Healy. 2012. *Analysis of radio-propagation environments to support standards development for RF-based electronic safety equipment.* US Department of Commerce, National Institute of Standards and Technology ....
[50] Yidong Ren, Puyu Cai, Jinyan Jiang, Jialuo Du, and Zhichao Cao. 2023. Prism: High-throughput LoRa backscatter with non-linear chirps. In *IEEE INFOCOM 2023-IEEE Conference on Computer Communications*. IEEE, 1–10.
[51] Yidong Ren, Amalinda Gamage, Li Liu, Mo Li, Shigang Chen, Younsuk Dong, and Zhichao Cao. 2024. Sateriot: High-performance ground-space networking for rural iot. In *Proceedings of the 30th Annual International Conference on Mobile Computing and Networking*. 755–769.

[52] Yidong Ren, Li Liu, Chenning Li, Zhichao Cao, and Shigang Chen. 2022. Is lorawan really wide? fine-grained lora link-level measurement in an urban environment. In *2022 IEEE 30th International Conference on Network Protocols (ICNP)*. IEEE, 1–12.

[53] Yidong Ren, Wei Sun, Jialuo Du, Huaili Zeng, Younsuk Dong, Mi Zhang, Shigang Chen, Yunhao Liu, Tianxing Li, and Zhichao Cao. 2024. Demeter: Reliable Cross-soil LPWAN with Low-cost Signal Polarization Alignment. In *Proceedings of the 30th Annual International Conference on Mobile Computing and Networking*. 230–245.

[54] Longfei Shangguan and Kyle Jamieson. 2016. Leveraging electromagnetic polarization in a two-antenna whiteboard in the air. In *Proceedings of the 12th International on Conference on emerging Networking EXperiments and Technologies*. 443–456.

[55] Chenglong Shao and Osamu Muta. 2024. TONARI: Reactive Detection of Close Physical Contact Using Unlicensed LPWAN Signals. *ACM Trans. Internet Things* 5, 2, Article 13 (apr 2024), 30 pages. https://doi.org/10.1145/3648572

[56] Leming Shen, Qiang Yang, Kaiyan Cui, Yuanqing Zheng, Xiao-Yong Wei, Jianwei Liu, and Jinsong Han. 2024. FedConv: A Learning-on-Model Paradigm for Heterogeneous Federated Clients. In *Proceedings of the 22nd Annual International Conference on Mobile Systems, Applications and Services*. 398–411.

[57] Leming Shen, Qiang Yang, Yuanqing Zheng, and Mo Li. 2025. AutoIOT: LLM-Driven Automated Natural Language Programming for AIoT Applications. In *Proceedings of the 31st Annual International Conference on Mobile Computing and Networking*.

[58] Yihang Song, Li Lu, Jiliang Wang, Chong Zhang, Hui Zheng, Shen Yang, Jinsong Han, and Jian Li. 2023. {$\mu$Mote}: enabling passive chirp de-spreading and {$\mu$W-level}{Long-Range} downlink for backscatter devices. In *20th USENIX symposium on networked systems design and implementation (NSDI 23)*. 1751–1766.

[59] Zhipeng Song, Shuai Tong, and Jiliang Wang. 2023. LoSense: Integrated Long-Range Sensing and Communication with LoRa Signals. In *2023 IEEE 31st International Conference on Network Protocols (ICNP)*. IEEE, 1–11.

[60] The Things Network. 2023. *Device Classes*. https://www.thethingsnetwork.org/docs/lorawan/classes/

[61] Xu Tian, Joseph Sarkis, Wei Chen, Yong Geng, Haozhi Pan, Zuoxi Liu, and Sergio Ulgiati. 2024. Greening the Belt and Road Initiative: Evidence from emergy evaluation of China's provincial trade with ASEAN countries. *Fundamental Research* 4, 2 (2024), 379–393. https://doi.org/10.1016/j.fmre.2022.11.007

[62] Shuai Tong, Yangliang He, Yunhao Liu, and Jiliang Wang. 2022. De-spreading over the air: long-range ctc for diverse receivers with lora. In *Proceedings of the 28th Annual International Conference on Mobile Computing and Networking*. 42–54.

[63] Shuai Tong, Zilin Shen, Yunhao Liu, and Jiliang Wang. 2021. Combating link dynamics for reliable lora connection in urban settings. In *Proceedings of the 27th Annual International Conference on Mobile Computing and Networking*. 642–655.

[64] Shuai Tong, Jiliang Wang, Jing Yang, Yunhao Liu, and Jun Zhang. 2023. City-wide LoRa Network Deployment and Operation: Measurements, Analysis, and Implications. In *Proceedings of the 21st ACM Conference on Embedded Networked Sensor Systems*. 362–375.

[65] Roman Trüb, Reto Da Forno, Andreas Biri, Jan Beutel, and Lothar Thiele. 2023. LSR: Energy-Efficient Multi-Modulation Communication for Inhomogeneous Wireless IoT Networks. *ACM Trans. Internet Things* 4, 2, Article 10 (apr 2023), 36 pages. https://doi.org/10.1145/3579366

[66] John L Volakis. 2007. *Antenna engineering handbook*. McGraw-Hill Education.

[67] Han Wang, Yihang Song, Qianhe Meng, Zetao Gao, Chong Zhang, and Li Lu. 2024. Sisyphus: Redefining Low Power for LoRa Receiver. In *Proceedings of the 30th Annual International Conference on Mobile Computing and Networking*. 1177–1191.

[68] Kun Wang, Jiani Cao, Zimu Zhou, and Zhenjiang Li. 2024. Swapnet: Efficient swapping for dnn inference on edge ai devices beyond the memory budget. *IEEE Transactions on Mobile Computing* 23, 9 (2024), 8935–8950.

[69] Song Wang, Jingqi Huang, and Xinyu Zhang. 2020. Demystifying millimeter-wave V2X: Towards robust and efficient directional connectivity under high mobility. In *Proceedings of the 26th annual international conference on mobile computing and networking*. 1–14.

[70] Yuting Wang, Xiaolong Zheng, Liang Liu, and Huadong Ma. 2022. Polartracker: Attitude-aware channel access for floating low power wide area networks. *IEEE/ACM Transactions on Networking* 30, 4 (2022), 1807–1821.

[71] Xianjin Xia, Qianwu Chen, Ningning Hou, and Yuanqing Zheng. 2022. Hylink: Towards high throughput lpwans with lora compatible communication. In *Proceedings of the 20th ACM Conference on Embedded Networked Sensor Systems*. 578–591.

[72] Xianjin Xia, Qianwu Chen, Ningning Hou, Yuanqing Zheng, and Mo Li. 2023. XCopy: boosting weak links for reliable LoRa communication. In *Proceedings of the 27th Annual International Conference on Mobile Computing and Networking*. 670–683.

[73] Xianjin Xia, Ningning Hou, Yuanqing Zheng, and Tao Gu. 2023. Pcube: scaling lora concurrent transmissions with reception diversities. *ACM Transactions on Sensor Networks* 18, 4 (2023), 1–25.

[74] Xianjin Xia, Yuanqing Zheng, and Tao Gu. 2019. FTrack: Parallel decoding for LoRa transmissions. In *Proceedings of the 17th Conference on Embedded Networked Sensor Systems*. 192–204.

[75] Zhenqiang Xu, Pengjin Xie, Jiliang Wang, and Yunhao Liu. 2022. Ostinato: Combating lora weak links in real deployments. In *2022 IEEE 30th International Conference on Network Protocols (ICNP)*. IEEE, 1–11.

[76] Yuan Yan and Yasamin Mostofi. 2016. Efficient clustering and path planning strategies for robotic data collection using space-filling curves. *IEEE Transactions on Control of Network Systems* 4, 4 (2016), 838–849.

[77] Kang Yang, Yuning Chen, Xuanren Chen, and Wan Du. 2023. Link quality modeling for lora networks in orchards. In *Proceedings of the 22nd International Conference on Information Processing in Sensor Networks*. 27–39.

[78] Kang Yang, Yuning Chen, and Wan Du. 2024. OrchLoc: In-orchard localization via a single LoRa gateway and generative diffusion model-based fingerprinting. In *Proceedings of the 22nd Annual International Conference on Mobile Systems, Applications and Services*. 304–317.

[79] Kang Yang and Wan Du. 2022. LLDPC: A low-density parity-check coding scheme for LoRa networks. In *Proceedings of the 20th ACM Conference on Embedded Networked Sensor Systems*. 193–206.

[80] Kang Yang, Miaomiao Liu, and Wan Du. 2024. : Rateless-Enabled Link Adaptation for LoRa Networking. *IEEE/ACM Transactions on Networking* (2024).

[81] Shiming Yu, Xianjin Xia, Ningning Hou, Yuanqing Zheng, and Tao Gu. 2024. Revolutionizing LoRa Gateway with XGate: Scalable Concurrent Transmission across Massive Logical Channels. In *Proceedings of the 30th Annual International Conference on Mobile Computing and Networking*. 482–496.

[82] Shiming Yu, Xianjin Xia, Ziyue Zhang, Ningning Hou, and Yuanqing Zheng. 2024. FDLoRa: Tackling Downlink-Uplink Asymmetry with Full-duplex LoRa Gateways. In *Proceedings of the 22nd ACM Conference on Embedded Networked Sensor Systems*. 281–294.

[83] Fusang Zhang, Jie Xiong, Zhaoxin Chang, Junqi Ma, and Daqing Zhang. 2022. Mobi2Sense: empowering wireless sensing with mobility. In *Proceedings of the 28th Annual International Conference on Mobile Computing And Networking*. 268–281.

[84] Yue Zhang and Lin Dai. 2020. On the optimal placement of base station antennas for distributed antenna systems. *IEEE Communications Letters* 24, 12 (2020), 2878–2882.

[85] Anfu Zhou, Shaoqing Xu, Song Wang, Jingqi Huang, Shaoyuan Yang, Teng Wei, Xinyu Zhang, and Huadong Ma. 2019. Robot navigation in radio beam space: Leveraging robotic intelligence for seamless mmwave network coverage. In *Proceedings of the Twentieth ACM International Symposium on Mobile Ad Hoc Networking and Computing*. 161–170.

[86] Lipeng Zhu, Wenyan Ma, and Rui Zhang. 2023. Movable Antennas for Wireless Communication: Opportunities and Challenges. *arXiv preprint arXiv:2306.02331* (2023).